Journal of Renewable Energies 24 (2021) 25 – 39 - **DOI:** https://doi.org/10.54966/jreen.v24i1.971

Journal of Renewable Energies

Revue des Energies Renouvelables

journal home page : https://revue.cder.dz/index.php/rer

Research Paper

Numerical Optimization of a Tandem Solar Cell based on $In_xGa_{1-x}N$

François Beceau Pelap [a], Eric Konga Tagne [a], Abraham Dimitri Kapim Kenfack [a,*]

[a] *UR de Mécanique et de Modélisation des systèmes physique (UR-2MSP), BP 69 Dschang, Dschang, Cameroun*

ARTICLE INFO

Article history:
Received 15 March 2021
Accepted 18 May 2021

Keywords:
Fraction of indium
Optical parameters
Electric power
Solar cell
Tandem
Efficiency

ABSTRACT

This article examines the best fraction of indium (x) and critical depth (H) of a single junction tandem photovoltaic (PV) cell (InxGa1-xN) in the vein to optimize its electrical efficiency. For better investigation, the optical and electronics parameters of a solar cell are determined as a function of the indium fraction and depth of the solar cell, leading to the resolution of the continuity equation and the establishment of the electrical characteristics (short circuit photocurrent, open-circuit photovoltage, maximum electric power). The outlet of our numerical investigations conducted under standard test conditions in the visible spectrum bandwidth of the irradiation, we found that the best indium fraction and the solar cell depth at the optimum electric power point are x=0.6 and H=1µm (In0.6Ga0.4N) respectively. Furthermore under normalized irradiation condition (0.1 W/cm2, T=25oC), we found a maximum electric power and efficiency of about 28.53 mW/cm2 and 28.53% respectively.

1. Introduction

The renewable energy sector has a huge potential to provide energy services for the world. In this regard, this sector must be constantly improved to satisfy energy demand. Further to the lack of energy in the worldwide, the research of a new alternative source of energy should be

* *Corresponding author, E-mail address: kapimdimitri347@gmail.com*
Tel.: +237 673218632

ISSN: 1112-2242 / EISSN: 2716-8247

developed. Fortunately, the solar cell cannot only meet our expectations of lack of energy but also solve the problem of climate change. Thus, because of its low efficiency, researchers paid a lot of attention to it and achieved an efficiency of 20 %. However, this efficiency is still insufficient, and therefore several optimization techniques such as doping [1], non-linearity [2-4], the use of ferromagnetic material [5] to name a few have been exposed in detail. Some authors have explored how to change the bandgap energy of material in the vein to improve the spectral sensitivity of the solar cell.

Fortunately, various studies on solar cells using nitrides semiconductors in solar cell applications have been done. Among them, the InGaN alloy appears as a promising candidate for photovoltaic applications because of its high tolerance to radiation, high mobility, and large absorption. Moreover, direct bandgap energy can be adjusted according to the fraction of indium. Thus, the bandgap energy of InGaN can be tuned from $0.7eV$ to $3.42eV$, covering approximately the total solar spectrum. In fact, it possible to have a different bandgap of energy by changing the fraction of indium named by x in this type of solar cell ($In_xGa_{1-x}N$) to have a good output. In this perspective, for a given value of the fraction of indium $x = 0.65$ Zhang *et al.* [6] modeled a solar cell $In_{0.65}Ga_{0.35}N$ and they achieved a conversion efficiency of 20.28%. However, for a solar cell with an Indium fraction of $x = 0.53$, Bouzid and Ben [7] have reached an efficiency of 24.88%. The same solar cell was improved in 2012 by Bouzid and Hamlaoui [8] in which they achieved an efficiency of 25.16%. Benmoussa *et al.* [9] considered an indium fraction $x = 0.52$ and obtained an efficiency of 22.99%. In 2014, Akter [10] reached an efficiency of 25.02% by considering an Indium fraction of $x = 0.64$. Recently, Mesrane *et al.* [11] achieved an efficiency of 26.50% for an indium fraction $x = 0.622$. As we can observe, these works mentioned reflect a great desire to improve the efficiency of this type of solar cell ($In_xGa_{1-x}N$). Their methods were essentially based on the random attribution of a fraction of indium, to deduce the efficiency of the solar cell. Motivated by the same objective and taking the operational method, we plan to appropriately optimize the performances of this type of solar cell $\left(In_xGa_{1-x}N\right)$. The operational method consisting of using the algorithm of Newton Raphson in order to determine the best fraction of indium and the depth of the solar cell such that, the efficiency of the solar cell is maximal. The algorithm of Newton Raphson is chosen within our investigation because of its robustness in the resolution of the nonlinear systems of equations. This algorithm is fast and assures a fast convergence toward the solution of the considered system of equations.

The work is organized as follows. In section 2, the illustration of a PV cell is presented. The determination of the optical and electronics parameters of a solar cell as a function of indium fraction and solar cell depth is carried out, leading to the resolution of the continuity equation and the establishment of the photocurrent, photovoltage electric power. In section 3, we study numerically the impacts of the fraction of indium and the depth of the solar cell on the short circuit photocurrent, open-circuit photovoltage, maximum electric power, efficiency, and fill factor. Section 4 is essentially devoted to the conclusion and suggestions.

2. Development of the model

2.1 Description of the solar cell

Figure 1 illustrates a PV module consisting of N_p branches, each containing N_s cells connected in series. We assume that the lighting is uniform on the PV module and that the generation rate of the carriers depends solely on the depth of the solar cell and the wavelength [12]. However as a PV cell is the unitary structure of a PV module, this allowed us to conduct the study on a solar cell.

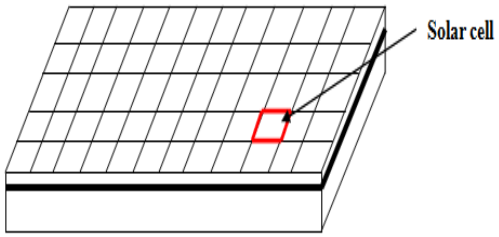

Fig 1. Illustration of a PV module [13]

In this study, we consider a solar cell as shown in Fig 2. The quantity H designates the depth of the solar cell. In practice, the dimensions of the base along the x and y axes are very large compared to the depth of the solar cell.

Thus, the current is neglected through these directions. During our investigations, the diffusion coefficient of the minority carriers in the emitter is considered negligible compared to that of the base [14]. Thus, our analysis is only developed at the base of the solar cell.

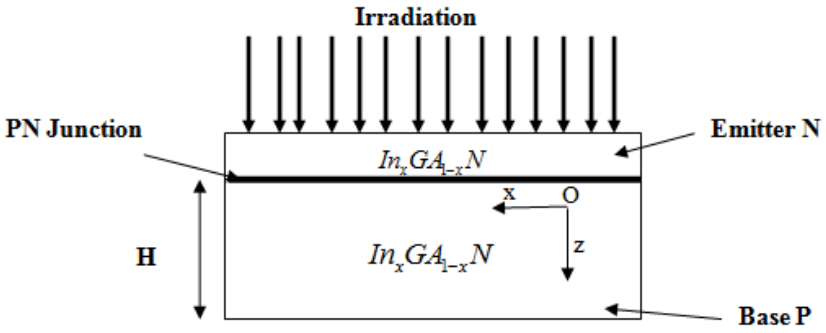

Fig 2. Presentation of a PV cell subjected to a uniform irradiation [11]

2.2 Determination of the parameters

2.2.1 Optical parameters

The solar cell used throughout our study is based on ($In_xGa_{1-x}N$), in which the grandeur x represents the fraction of Indium. The bandgap energy of the solar is related to the fraction of Indium as follows [15].

$$Eg = x \cdot Eg^{InN} + (1-x) \cdot Eg^{GaN} - b \cdot x \cdot (1-x) \tag{1}$$

wherein the bandgap energy of $InN\left(Eg^{InN}\right)$ and $GaN\left(Eg^{GaN}\right)$ are respectively $0.7eV$ and $3.42eV$; b is the bowing parameter $(b = 1.43eV)$. The absorption coefficient is also related to the fraction of indium and the incident photon as follows [16].

$$\alpha(\lambda, x) = 10^5 \sqrt{C(x)\left(E_{ph} - E_g(x)\right) + D(x)\left(E_{ph} - E_g(x)\right)^2} \tag{2}$$

wherein $E_{ph} = 1.24/\lambda$ represents the energy of the photon in which λ is the wavelength,

$C = 3.525 - 18.29 \cdot x + 40.22 \cdot x^2 - 37.52 \cdot x^3 + 12.77 \cdot x^4$; $D = -0.6651 + 3.616 \cdot x - 2.46 \cdot x^2$

The refractive index of the solar cell is also related to the incident energy of the photon and the fraction of indium as follows [17].

$$N(\lambda, x) = \sqrt{A(x) \cdot \left(E_g / E_{ph}\right)^2 \cdot \left[2 - \sqrt{1 + E_{ph}/E_g} - \sqrt{1 - E_{ph}/E_g}\right] + B(x)} \tag{3}$$

wherein $A = 13.55 \cdot x + 9.31 \cdot (1-x)$; $B = 2.05 \cdot x + 3.03 \cdot (1-x)$

2.2.2 Electronics parameters

The intrinsic carrier concentration is also linked to the fraction of indium and takes the following form [11].

$$n_i = \sqrt{N_C \cdot N_V} \cdot e^{\frac{-Eg}{2 \cdot Kb \cdot T}} \tag{4}$$

In which the density of state in the conduction band and valence band are expressed as follows $N_C = \left(0.9 \cdot x + 2.3 \cdot (1-x)\right) \cdot 10^9$ and $N_V = \left(5.3 \cdot x + 1.8 \cdot (1-x)\right) 10^{19}$ respectively. The quantities K_b and T are respectively the Boltzmann coefficient and the temperature. The effective mass of carriers is express as follows [11].

$$m_n = \left(0.12 \cdot x + 0.2 \cdot (1-x)\right) m_o \tag{5}$$

wherein, m_o is the mass of the elementary charge. Knowing the link between the mobility of the carriers and the effective masse expressed by $\mu = q \cdot \tau / m_n$, the diffusion coefficient used within our simulations is express as follows:

$$D = \frac{K_b \cdot \tau \cdot T}{\left(0.12 \cdot x + 0.2 \cdot (1-x)\right) m_o} \tag{6}$$

wherein q and τ represent respectively the elementary charge and lifetime of the carriers

2.2.3 Electrical parameters

The equation governing the distribution of minority carriers n_λ within the base of the solar cell is express as follows [5].

$$\frac{\partial^2 n_\lambda}{\partial^2 z} - \frac{n_\lambda}{L^2} = -\frac{G(z,\lambda)}{D} \tag{7}$$

n_λ represents the density of minority carrier per unit of wavelength,

$G(z,\lambda) = \phi_o(\lambda) \cdot \alpha(\lambda) \cdot \left(1 - R(\lambda)\right) \cdot e^{-\alpha(\lambda) \cdot z}$ represents the generation rate of carrier per unit of wavelength,

wherein $\phi_o(\lambda)$, represents the density of photon per unit of wavelength, $\alpha(\lambda)$ the absorption coefficient, $R(\lambda)$ the reflection coefficient [12].

Then, the general solution of Eq. (7) takes the following form:

$$n_\lambda(z,H,x,) = Q(\lambda)\cosh\left(\frac{z}{L}\right) + F(\lambda)\sinh\left(\frac{z}{L}\right) + \beta e^{-\alpha z} \tag{8}$$

in which $\beta(\lambda) = -\phi_o(\lambda)(1-R(\lambda))\alpha(\lambda)\cdot L^2 \Big/ \{D(\alpha^2\cdot L^2 - 1)\}$ and $L = \sqrt{D\cdot\tau}$ represents the diffusion length. The coefficients Q and F are determined by exploiting the upcoming boundary conditions [17].

- At the PN junction of the solar cell :

$$D\frac{\partial n_\lambda}{\partial z} = S_f \cdot n_\lambda \qquad z = 0 \tag{9a}$$

- At the back side of the solar cell :

$$D\frac{\partial n_\lambda}{\partial z} = S_f \cdot n_\lambda \qquad z = H \tag{9b}$$

In relation (9a), the quantity S_f represents the speed of recombination of the carriers at the PN junction. It model the flux of minority carried that cross the PN junction in the vein to contribute to the formation of the current. Throughout this work, the solar cell is considered ideal. Meanwhile, the internal losses like the intrinsic recombination speed of the minority carriers at the PN junction are neglected. Then, only the extrinsic recombination speed imposed by an external load resistance is considered within our investigations [18].

In relation (9b), the quantity S_b defines the speed of recombination of the carriers effectively recombined at the back surface of the cell [19]. Then the total carrier generated per unit volume in the bandwidth of the incident spectrum of light capable to be absorbed by the solar cell is expressed as follows:

$$n(z,H,x,S_f) = \int_{\lambda_{\min}}^{\lambda_{\max}} n_\lambda d\lambda \tag{10}$$

wherein $\lambda_{\min}$ defines the minimal wavelength of light and $\lambda_{\max} = 1.24/Eg$

2.2.3.1 Photocurrent

The photocurrent delivered by the solar cell depends on the speed of recombination, the fraction of indium, and the depth of the solar cell. It expressed as follows [20, 21]

$$I_{ph}\left(x,H,S_f\right)=q\cdot D\cdot\left.\frac{\partial n}{\partial z}\right|_{z=0} \tag{11}$$

By taking into account the boundary condition, the photocurrent is express as follows:

$$I_{ph}\left(x,H,S_f\right)=q\cdot S_f\cdot\left[\int_{\lambda_{\min}}^{\lambda_{\max}}Q\left(x,H,\lambda,S_f\right)d\lambda+\int_{\lambda_{\min}}^{\lambda_{\max}}\beta(\lambda)d\lambda\right] \tag{12}$$

While taking the fraction of indium as parameter within our investigation, the short circuit photocurrent is obtained when the speed of recombination is very large. Thus we have:

$$I_{sc}\left(x,H\right)=\lim_{S_f\to+\infty}I_{ph} \tag{13}$$

2.2.3.2 Photovoltage

From Boltzmann's law, photovoltage at the outer charge terminals is given by [22, 23, 24]:

$$V_{ph}\left(x,S_f,H\right)=V_t\cdot\log\left(\frac{N_b}{n_i^2}n\left(z,x,S_f,H\right)+1\right)\Bigg|_{z=0} \tag{14}$$

Where N_b is the impurity level. The quantity $V_t=A\cdot K_b\cdot T/q$ designates the thermal voltage in which A, T K_b and q stand for the ideal factor, the temperature, the Boltzmann factor, and the elementary charge, respectively. By considering the total wavelength capable to be absorbed by the solar cell, we have:

$$V_{ph}\left(x,S_f,H\right)=V_t\cdot\log\left(\frac{N_b}{n_i^2}\left[\int_{\lambda_{\min}}^{\lambda_{\max}}Q\left(x,H,\lambda,S_f\right)d\lambda+\int_{\lambda_{\min}}^{\lambda_{\max}}\beta(\lambda)d\lambda\right]+1\right) \tag{15}$$

The open circuit photovoltage is obtained when the speed of recombination of carrier turns to zero. Hence:

$$V_{oc}\left(x,H\right)=\lim_{S_f\to0}V_{ph} \tag{16}$$

2.2.3.3 Electric power

The electric power collected at the terminals of the solar cell results from the product between the photocurrent and the photovoltage [12] is written as:

$$P_{ph}\left(S_f, x, H\right) = I_{ph}\left(S_f, x, H\right) \cdot V_{ph}\left(S_f, x, H\right) \tag{17}$$

Form this latter, the efficiency is express as follows:

$$P_{\max}\left(x, H\right) = Max\left(P_{ph}\left(x, H, S_f\right)\right) \tag{18}$$

In the vein to optimize that maximum electric power harvested from the solar cell, the depth and the fraction of indium should satisfy the following condition.

$$\overrightarrow{grad}\left(P_{\max}\left(x, H\right)\right) = \vec{0} \tag{19}$$

Then finally, the optimal depth (H_{op}) and fraction of indium (x_{op}) verify this nonlinear system of equation expresses as follows:

$$\begin{cases} \dfrac{\partial P_{\max}\left(x, H\right)}{\partial x} = 0 \\ \dfrac{\partial P_{\max}\left(x, H\right)}{\partial H} = 0 \end{cases} \tag{20}$$

Fortunately, the algorithm of Newton Raphson for a system of non-linear functions allows us to obtain numerical values of the two grandeurs with the aim the get the maximum power. The algorithm of Newton Raphson is chosen because of its robustness in the resolution of the nonlinear systems of equations. This algorithm is fast and assures a fast convergence toward the solution of the considered system of equations.

3. Results and discussion

3.1 Effect of the fraction of indium and the depth on the short circuit photocurrent

The simulations of the short circuit photocurrent by exploiting the analytical expression (13) are conducted in this part. We proceed to the presentation of the variation of the short circuit photocurrent against the fraction of Indium (x) for various depth of the solar cell depicted in Fig.3(a) on one hand, and against the depth for a various fraction of Indium displayed in Fig.3(b) on the other hand. The simulations are made under standard tests where the irradiation is normalized at P_{in}=0.1W/cm^2 and the temperature is 25°C. The system parameters considered throughout of our simulations are: $\tau = 6.5 ns$, $S_b = 10^2\ cm/s$, $N_b = 10^{19}$ [11].

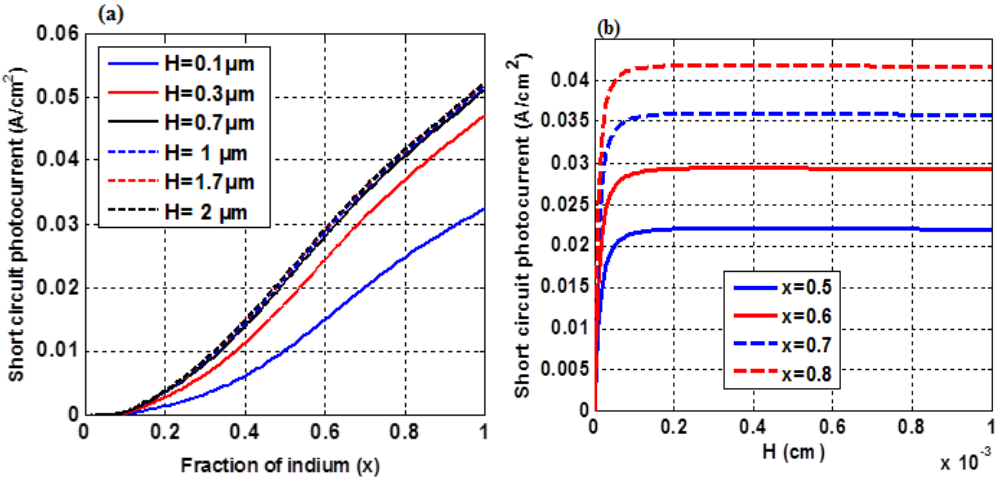

Fig 3. Short circuit photocurrent versus **a)** fraction of indium for various depths of the solar cell; **b)** depth of solar cell for a various fraction of indium. The short circuit photocurrent varies strongly with the fraction of indium for various depths while it remains constant with the depth of solar cell for various fractions of indium.

The visible light spectrum chosen throughout our investigations is delimited by the bandwidth $\lambda_{\min} = 0.4\,\mu m$ and $\lambda_{\max} = 1.24/Eg$ coincides approximately with the bandgap energy of this solar cell defined between $0.7\,eV$ and $3.42\,eV$. The simulation results for a case of a solar cell are considered. We remark on Fig 3(a) that for the fraction of indium between $[0;0.1[$, the short circuit photocurrent is almost zero. Meaning that, when the solar cell has a fraction of indium in the above-mentioned range, it becomes insensitive to the incident photon and therefore the solar cell does not produce current. Otherwise, the bandgap energy of the material is far greater than the energy of the incident photon. Hence, the photovoltaic effect does not take place and therefore, no current is produced. In contrast, for the indium fraction beyond 0.1, the solar cell starts to produce current. Indeed in that zone, the bandgap of energy of the solar cell has drastically reduced and become sensitive to the spectrum of light. Thus, as the bandgap energy of the solar cell decreases, the number of carriers generated increases too, and therefore the short circuit photocurrent of the solar cell increases. We also remark that the solar cell depends strongly on its depth, observed by the fast increases of the short circuit photocurrent. Furthermore, beyond a depth of 0.1µm, the output photocurrent does not depend on the depth of the solar cell. Meaning that beyond $1\,\mu m$, the maximum carriers able to produce a photocurrent in a solar cell have been all extracted. Somewhere in Fig 3(b), we remark that the photocurrent strongly depends also on the depth and turns towards an asymptotic value.

Furthermore, these asymptotic value increases with the fraction of indium. Meaning that to get a maximum photocurrent within the process of manufacturing the solar cell, the depth of the solar cell should be chosen small as possible.

3.2 Impact of the fraction of indium and depth on the open circuit photovoltage

Due to the standard test conditions, numerical simulations of the mathematical expression (16) are performed with the parameters of Fig. 3 and displayed in Fig. 4. The evolution of the open-circuit photovoltage collected on a solar cell is plotted against the fraction of Indium (x) for various depths of the solar cell and depicted in Fig.4(a) on one hand and versus depth for various fractions of indium and depicted in Fig. 4(b) on the other hand. We note in Fig. 4(a) that for a fraction of indium less than 0.1, the solar cell does not produce photovoltage. Showing that in this zone, the carriers are not yet generated because of the smallness of the energy of the incident photon compared to the bandgap energy of the solar cell. Somewhere, beyond 0.1, the behavior of the solar cell has changed.

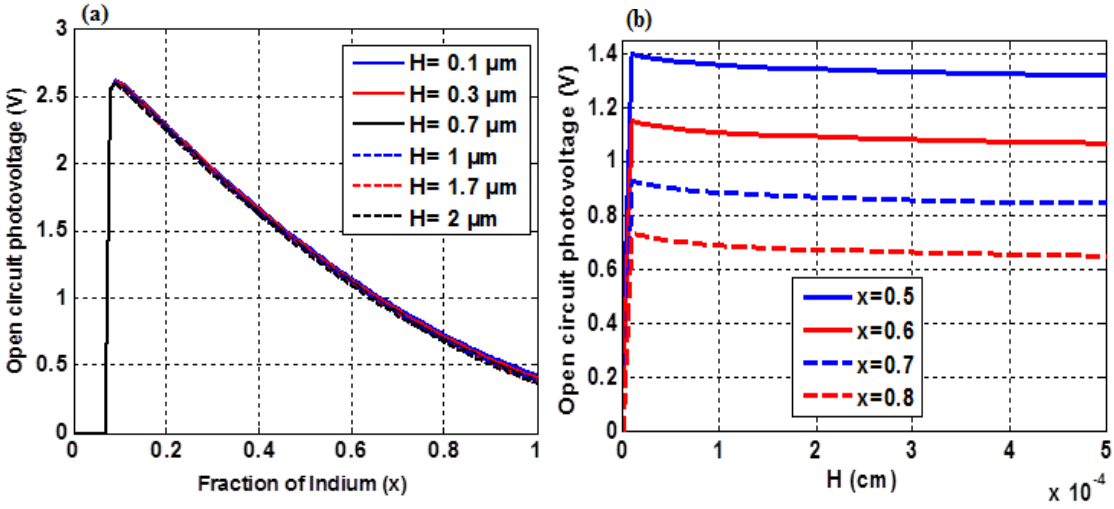

Fig 4. The open-circuit photovoltage versus **a)** fraction of indium for various depths of the solar cell; **b)** depth of solar cell for various fractions of indium. The open-circuit photovoltage decreases with the fraction of indium but is lightly affected by the depth of the solar cell.

We note a drastic increase of the open-circuit photovoltage from 0 to 2.6 V. In fact, that drastic increase of the photovoltage is because an important amount of carriers excited stands at the PN junction. From the short circuit photocurrent, very few of those carriers standing at the PN

junction have sufficient energy to cross the PN junction. Thus, when the fraction of indium increases, the number of carriers capable to produce the current increases too. Then, the number of carriers standing at the PN junction reduces and therefore reduces the open photovoltage. Somewhere in Fig 4(b), we remark that the photocurrent does depend on the depth. Meaning that for a fixed fraction of indium and also in the aim to avoid the wastage of the material and collect a maximum voltage, the depth of the solar cell should be small as possible.

3.3 Contribution of the fraction of indium and depth on the maximum electric power

In this part, the variations of the maximum electric power are plotted by exploiting expression (18) with the system parameter of Fig.3. The results of our simulations are presented in Fig.5. It clearly appears in Fig.5(a) that, for the fraction of indium less than 0.1, the maximum electric power of the solar cell is zero.

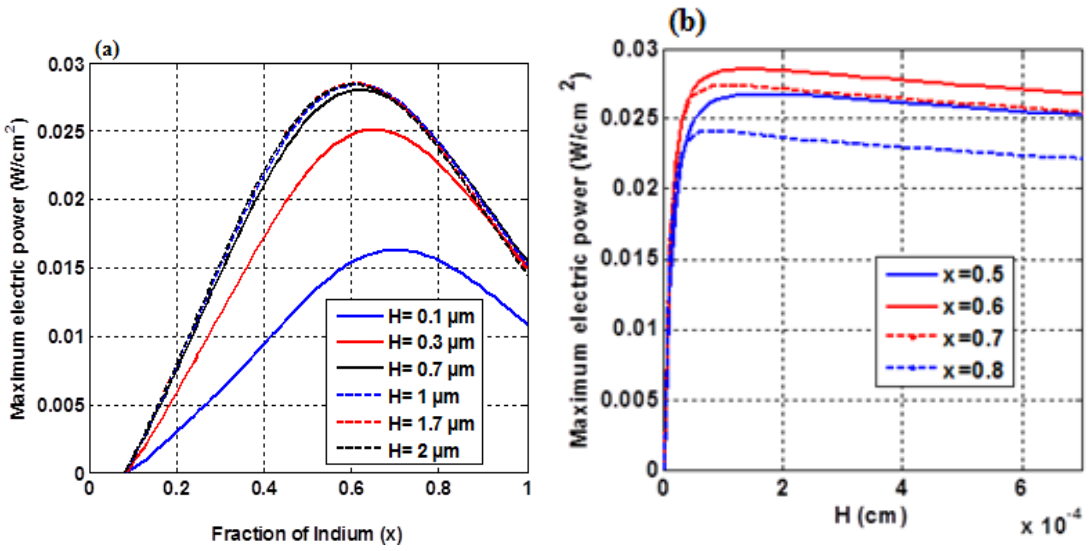

Fig 5. Variation of the maximum electric power versus **a)** fraction of indium for various depths of the solar cell, **b)** depth of the solar cell for various fractions of indium.

Meaning that the solar cell does not operate. In contrast, beyond 0.1, we note that the maximum electric power increases pass through a turning point corresponding to an optimal fraction of indium and decreases after. In fact, beyond 0.1, the solar cell starts to operate fully. Meaning that the solar cell is sensitive to the wavelength and therefore the carriers are extracted from the solar cell up to the turning point. However, beyond the turning point, the indium fraction becomes harmful to the solar cell. It induces losses of energy of the minority carriers by increasing the process of recombination which occurs strongly in the solar cell. On the same figure, we also remark that the turning point increases with the depth of the solar cell.

Furthermore, beyond 1µm as the depth of the solar cell, the maximum power does not vary significantly. Meaning that the maximum carriers able to be extracted from the solar cell are achieved when the depth of the solar cell is around 1µm. Somewhere, Fig.5(b) shown that the optimal maximum electric power strongly depends on the depth of the solar cell. By using the algorithm of Newton Raphson for the nonlinear system (20), the parameters of a solar cell obtained at the optimal point are recorded in Table 1. Thus, we note that the maximum power delivered by the solar cell at the optimum point is achieved when x_{op}=0.6at H_{op}=1µm.
Thus in the line to optimize the photosensitivity of this type of solar cell, the optimal fraction of indium and the depth of the solar cell is $x = 0.6$, and $H = 1.4\mu m$ respectively.

Table1. Numerical data collected at the optimal point of maximum electric power

Quantity at the optimal point	Corresponding value
Depth $H_{op}(\mu m)$	1.4
Maximum electric power $\left(mW / cm^2\right)$	28.53
Maximum efficiency (%)	28.53
Fraction of Indium $\left(x_{op}\right)$	0.6
Open circuit photovoltage $V_{oc}(V)$	1.1
Short circuit photocurrent $I_{sc}\left(mA / cm^2\right)$	30
Fill factor FF (%)	86.45

Hence the formula becomes $In_{0.6}Ga_{0.4}N$. This new configuration of the solar cell offers the best conversion efficiency of a single junction of the solar cell of about 28.53% compared to Mesrane *et al.* [11] in which they obtained 26.50%.

4. Conclusion

The content of this work was essentially based on the numerical optimization of the new generation of solar cells made on $In_xGa_{1-x}N$. Our investigation was focused on the determination of the optimal fraction of indium (x) and depth (H) of the solar cell in the vein to get the best maximum electric power delivered by a solar cell. Both analytical and numerical investigation was carried out on the electrical quantities (short circuit photocurrent, open-circuit photovoltage, electric power). Many important results are established. The short circuit photocurrent increases with the fraction of indium while the open-circuit photovoltage decrease. Furthermore, by using the algorithm of Newton Raphson, the values of indium fraction and depth of solar cell at the optimal electric power are respectively x=0.6 $x = 0.6$ and H=1µm,

which allows us to achieve an electrical efficiency of 28.53%. Hence, we note an increase of conversion efficiency of 2.03 % compared to the recent result obtained by Mesrane *et al* [11] in which they achieved 26.50%. These results obtained offer a new way to manufacturers of PV modules, a new architecture of the solar cell in the vein to significantly resolve the lack of energy.

Nomenclature

Parameters	Name
H	Depth of the solar cell
I_{ph}	Photocurrent
I_{sc}	Short circuit Photocurrent
P_{ph}	Electric power
PV	Photovoltaic
V_{ph}	Photovoltage
V_{oc}	Open circuit Photovoltage
S_f, S_b	Speeds of recombination
x	Fraction of indium

5. References

[1] Sane, M., Barro, F.I. (2015). Effect of both magnetic field and doping density on series and shunt resistance under the frequency. *Indian Journal of Pure Applied physics*, (53), 590-595.

[2] Dongo P.D., Kapim Kenfack A.D., Pelap, F.B. (2014). Effects of a thermal nonlinear resistance on the power output of the PV cell, *Journal of Energy Technologies and Policy*, (4), 100-111

[3] Pelap, F.B, Dongo, P.D, Kapim kenfack A.D. (2016). Optimization of the characteristics of the PV cells using nonlinear electronic components, *Sustainable Energy Technologies and Assessments*, (16) 84-92. http://dx.doi.org/10.1016/j.seta.2016.05.005

[4] Konga, E., Kapim Kenfack, A.D., Pelap, F.B. (2020)**.** Effect of a Thermal nonlinear absorption coefficient on the dynamics of photovoltaic panel, Journal of Energy Technologies and Policy, (10)**,** 9-15. http://dx.doi.org /10.7176/ JETP/10-6-02.

[5] Kapim Kenfack, A.D., Konga, T.E., Pelap, F.B. (2020). Behavior of a Ferromagnetic Photovoltaic Module under the Harmful Effects of an External Magnetic Field, *International Journal of Advanced Sciences and Technology*. (29), 14730-14745.

[6] Zhang, X., Wang, X., Xiao, H., Yang, C., Ran, J., Wang, C., Hou, Q., Li, J. (2007). Simulation of In0. 65Ga0. 35 N single-junction solar cell, *Journal of Physics D: Applied Physics*, (40), 56-95.

[7] Bouzid, F., & Machiche, S.B. (2011). Potentials of InxGa1-xN photovoltaic tandems, *Revue des Energies Renouvelables*, (14) 47-56.

[8] Bouzid, F., & Hamlaoui, L. (2012). Investigation of InGaN/Si double junction tandem solar cells, *Journal of Fundamental and Applied Sciences*, (4) 59-71.

[9] Benmoussa, D., Hassane, B., & Abderrachid, H. (2013). *Simulation of In0.52Ga0.48N solar cell using AMPS-1D*, Proceedings of the 1st International Renewable and Sustainable Energy Conference (IRSEC'13), 23–26, Morocco

[10] Akter, N. (2014). Design and simulation of Indium Gallium Nitride multijunction tandem solar cells, *International Journal of Research in Engineering and Technology*, (3), 315-321.

[11] Mesrane, A, Rahmoune, F, Mahrane, A, Oulebsir, A. (2015). Design and Simulation of InGaN P-N Junction Solar Cell, *International Journal of Photoenergy*, 1-9, http://dx.doi.org/10.1155/2015/594858

[12] Zerbo, I, Zoungrana, M, Ouedraogo, A, Korgo, B, Zouma, B, Bathiebo, D.J. (2014). Influence of electromagnetic waves produced by an amplitude modulation radio antenna on the electric power delivered by a silicon solar cell, *Global Journal of Pure and Applied Sciences*, (20), 139-148.

[13] Kapim Kenfack, A.D, Konga, T.E, Pelap, F.B. (2020). Contribution of a non-uniform magnetic field on the electric power of a photovoltaic panel, *Journal of Energy Technology and Policy*, (10), 16-29, http://dx.doi.org/10.7176/ JETP/10-7-03.

[14] Ly, I, Lemrabott, O.H, Dieng, B, Gaye, I, Gueye, S, Diouf, M.S, Sissoko, G. (2012). Techniques de détermination des paramètres de recombinaison et le domaine de leur validité d'une photopile bifaciale au silicium polycristallin sous éclairement multi spectral constant en régime statique. *Revue des Energies Renouvelables*, (15), 187-206.

[15] Nawaz, M., & Ahmad, A. (2012). A TCAD-based modeling of GaN/InGaN/Si solar cells, *Semiconductor Science and Technology*, (27) 49-51.

[16] Brown, G.F., Ager, J. W., Walukiewicz, W., Wu, J. (2010). Finite element simulations of compositionally graded InGaN solar cells, *Solar Energy Materials & Solar Cells*, (94), 478-483.

[17] Piprek, J. (2013). Semiconductor Optoelectronic Devices: Introduction to Physics and Simulation, Academic Press.

[18] Ndiaye , E.H., Sahin, G., Dieng, M., Thiam, A., Diallo, H.L., Ndiaye, M., Sissoko, G. (2015). Study of the intrinsic recombination velocity at the junction of silicon solar under Frequency modulation and illumination", Journal of Applied Mathematics and Physics, (3**)** 1522-1535.

[19] Zerbo, I., Zoungrana, M., Sourabie, I., Ouedraogo, A., Zouma, B., Bathiebo, D.J. (2015). External magnetic field effect on bifacial silicon solar cell's electric power and conversion efficiency, *Turkish Journal of Physics*, (39**)**, 288-294. https://doi.org/10.3906/fiz-1505-10

[20] Zoungrana, M., Zerbo, I., Soro, B., Savadogo, M., Tiedrebeogo, S., Bathiebo, D.J. (2017). The effect of magnetic field on the efficiency of a silicon solar cell under an intense light concentration, *Advance Science and Technology*, (11**)** 133-138.

[21] Moujtaba, M., Ndiaye, M., Diao, A., Thiame, M., Barro, I.F., Sissoko, G. (2012). Theoretical study of the influence of illumination on a silicon solar cell under multispectral illumination, *Research Journal of Applied Sciences Engineering and Technology*, (4), 5068-5073.

[22] Moussa, I.N., Diouf, M.S., Thiam, A., Ould E.M., & Sissoko, G. (2015) Influence of magnetic field on the capacitance of a vertical junction parallel solar cell in static regime under multispectral illumination, *International Journal of Pure and Applied Sciences and Technology*, (31), 65-75.

[23] Sane, M., Zoungrana, M., Diallo, H.L., Sahin, G., Thiam, N., Ndiaye, M., Dieng, M., Sissoko, G. (2013). Influence of incidence angle on the electrical parameters of a vertical silicon solar cell under frequency modulation, *International Journal of Inventive Engineering and Sciences*, (1), 37-40.

[24] Thiam, A., Sahin, G., Moujtaba, M., Mbow, B., Diouf, M.S., Ngom, M.I., Sissoko, G. (2015). Incidence angle effect on electrical parameters of a bifacial silicon solar cell illuminated by its rear side in frequency domain, *International Journal of Pure and Applied Sciences and Technology*, (30), 29-42.